

# Non-metallic inclusions and hook cracks of high-frequency induction welded pipes

*A. A. Kazakov, Dr. Eng., Prof., Head of “Metallurgical Examination” Lab.<sup>1</sup>,  
e-mail: kazakov@thixomet.ru;*

*D. V. Kiselev, Technical Director<sup>1</sup>;*

*V. A. Muryshev, Chief Specialist, Engineering and Technology Center<sup>2</sup>;*

*I. V. Rybalchenko, Head of the Lab. of Metal Science and Heat Treatment of Metals,  
Central Plant Laboratory<sup>2</sup>*

<sup>1</sup> Thixomet Ltd. (St. Petersburg, Russia)

<sup>2</sup> Vyksa Steel Works JSC (Vyksa, Russia)

Based on the analysis of foreign experience, it is shown that hook cracks are the most common defect of pipe joints obtained by high-frequency induction welding (HFIW). Particular attention is paid to the non-metallic inclusions (NMIs) that caused this defect. Their composition, origin and ways of elimination are considered. It was found that in the foreign literature the nature of certain oxides found in the vicinity of defects is often declared without objective evidence of their origin.

The interpretation technique of NMIs composition, which caused the formation of defects of pipe joints obtained by HFIW, is presented. This technique is a part of the "Metal products quality system", implemented on the basis of Thixomet image analyzer, working in the laboratories of Vyksa Steel Works JSC.

The compositions of NMIs found in the discontinuities of welded joint defects of 09G2S steel grade were interpreted using thermodynamic simulation of primary NMIs and generalized for two sets of 65 and 70 defects in each set. These compositions differ significantly from each other and correspond to the following indigenous inclusions:  $Al_2O_3$ ,  $MgO \cdot Al_2O_3$ , calcium aluminates, CaO and CaS. The same compounds can form exo-indigenous NMIs conglomerates after the interaction between liquid calcium aluminates and refractories based on MgO or  $ZrO_2$ , and/or mould powder. The unique ranges of concentration changes of the main elements included in individual phases and their combinations in NMIs conglomerates are used for automated determination of their origin when conducting metallographic examination of defects using the Thixomet image analyzer. Examples of using the origin of NMIs to find the exact place in the secondary steelmaking and steel casting technologies for their improvement and on this basis to improve the quality of HFIW pipe joints are also presented.

**Key words:** pipes, welding, high frequency induction welding, defects, hook cracks, non-metallic inclusions, thermodynamic simulation, indigenous, exogenous, interpretation.

**DOI:** 10.17580/cisr.2022.02.08

## Introduction

It is known that several types of defects are found in pipe joints obtained by high-frequency induction welding (HFIW), the most complete list of which is given in the “Technician ERW Weld Discontinuity Characterization Guide” [1]. With reference to API 5T1 [2], it specifies all possible types of discontinuities that are typical for this welding method: on bondline, lamination, crack, hook cracks etc. A detailed description is given for each of these defects, including: origination, advantageous location, parameters and unique properties, most possible way and driving forces of crack propagation, possibility of reveal, location scheme in welded joint and examples of defects images. However, despite such specification, there is absolutely no information about the origin of non-metallic inclusions, which caused the formation of the defects of HFIW pipe joints, that are actual for modern production.

There are descriptions of hook-shaped defects in few foreign publications [3–15]. National standards GOST 31447-2012 [16] and GOST 59496-2021 [17] provide only the

most common defects of welded joints without description of specific types typical for HFIW pipe joints. Meanwhile, as hydrostatic tests of such pipes have shown [3], the largest discontinuities of the base metal reduce their tensile strength by less than 25 %, while any defects in the welded joint reduce this strength by up to 50 %.

The authors of paper [4] investigated defects of more than 250,000 pipes detected by automated ultrasonic inspection system with sensitivity of 0.1 mm under conditions of POSCO operating production. They showed that the fraction of hook cracks reached 81%, and the rest were surface (16 %) and other (3 %) defects.

According to API 5T1 hook cracks are formed during metal separation along strings of non-metallic inclusions or segregation at the sheet edge. These defects are initially located parallel to the surface of the sheet, but during the upsetting of its edges in the process of pipe manufacturing they turn to the inner or more often to the outer diameter of the pipe [2]. Non-metallic inclusions as the root cause of these defects are listed not only in API documents [1–2], but also in all other literature [3–13].

The authors of [6, 7] and, following them, other researchers of nonmetallic inclusions inside hook cracks [8, 9] give the following descriptions of their origin. The presence of CaO and Al<sub>2</sub>O<sub>3</sub> in inclusions is associated with exogenous slag particles. If, along with CaO and Al<sub>2</sub>O<sub>3</sub>, inclusions additionally contain MgO, they are attributed to the products of interaction of slag and tundish refractories, and if additionally found CaS, they are attributed to the products of steel modification by calcium. The inclusions of the CaO-Al<sub>2</sub>O<sub>3</sub>-CaS system, which caused the formation of hook cracks, are located at the edges of the sheets, while the cracks formed in the center along the pipe thickness are associated with MnS and Al<sub>2</sub>O<sub>3</sub> [10]. Secondary oxidation of steel is associated with an increased content of Al<sub>2</sub>O<sub>3</sub>. The mechanism of steel contamination by exogenous inclusions is the result of a combination of chemical interaction and mechanical erosion of the refractories of the metal wiring [7]. Depending on the position of the rolls for edge upsetting, the depth and thickness of hook cracks can vary [11]. Hook cracks can be eliminated with optimal calcium treatment of the steel, improved argon stirring conditions in the ladle furnace, control of melt flows in the tundish and better quality of refractories for its fabrication [6].

In [11] the most complete description of all possible varieties of hook defects was made. We shall consider only those of them, which are caused by presence of non-metallic inclusions and are actual for modern HFIW pipe production.

Defects formed by non-metallic inclusions of steelmaking origin are detected on both diameters of the pipe if they are related to general steel contamination or only on its outer diameter if they were delivered to this area by flotation on argon bubbles or surfacing during slab solidification in a curved-type continuous caster.

The origin of cracks formed by entrapped mould powder is similar: only mould powder inclusions delivered by argon bubbles are detected on the outer side of the pipe, or on both pipe diameters if they have filled microcracks formed by the mould oscillation marks during formation of the solid shell of the ingot [8]. Narrow slab edges are under the maximum thermal stresses and are susceptible to the formation of micro-cracks at the edge of coils by oscillation marks. After cold forming of the sheets, small microcracks at the coil edges may open, then they are detected by ultrasonic inspection along the bondline. Some of them look like hook cracks. Cleaning the narrow edges of the slab to remove the microcracks from the mould oscillation marks results in a reduction of the associated defects in pipes obtained by HFIW [8].

Refractory materials of metal wiring are affected by a steel melt deoxidized with aluminum, which reacts with the easily reducible oxides FeO, MnO, TiO<sub>2</sub> and SiO<sub>2</sub>. On the refractory surface, impregnated with the products of this interaction, complex non-metallic inclusions are formed, which are separated from it together with the refractory particles and are captured by the melt. A similar reaction can take place with tundish slag containing reducible oxides. The excessive consumption of argon used to prevent clogging of the entry nozzle intensifies the processes of capturing all these inclusions and their consumption by the melt.

From the above analysis it follows that hook cracks are formed in the place of the weld joint *where the most intensive metal upsetting occurs, and only in the presence of coarse clusters of non-metallic inclusions at the sheet edges in these very places*. These two circumstances are necessary and sufficient conditions for the formation of discontinuities or laminations, which, following the lines of metal flow, deviate from the rolling direction to the outer or less often to the inner diameter of the pipe. In this way a hook or J-shaped form of the defect is formed. *Therefore, the absence of non-metallic inclusions in the zone of intensive edge upsetting can guarantee the formation of a defect-free welded joint.*

In the technical literature [3-15] the nature of certain oxides in the composition of NMIs found in the vicinity of defects is often stated without evidence of their origin, and these studies are based on single measurements of separate inclusions. For example, in [18] an attempt was made to find the source of the magnesia spinel, the composition of which was determined at one point of one of the inclusions found in the hook crack discontinuity. To determine the origin of MgO·Al<sub>2</sub>O<sub>3</sub>, the authors thoroughly studied hundreds of NMIs in each of the samples taken at all stages of secondary steelmaking and in finished coiled metal. To do so, they used the SEM-EDS method with automatic particle analysis (AFA). Among these hundreds of NMIs not a single inclusion of pure magnesia spinel was found: all of them were in a mixture with calcium aluminates, and the vast majority of deoxidation and modification products remaining in the finished coiled metal, after the steel treatment with calcium, were CaO-CaS in a mixture with calcium aluminates [18].

Earlier, we developed a "cluster" technique for interpretation of composition of nonmetallic inclusions found in discontinuities of HFIW welds, which allowed us *to summarize many years of factory experience in studying these defects in steels 09G2S [19] and 22GYu [20]*. Compositions of NMIs calculated by thermodynamic simulation were combined into the first type of clusters of indigenous deoxidation and modification products. Hundreds of compositions of real conglomerates of inclusions revealed in discontinuities of welded joints were combined into the second type of clusters. Comparing these two types of indigenous and real NMIs clusters, all real inclusions were divided into indi-exogenous and exo-indigenous depending on the dominated fraction of exogenous and indigenous NMIs in their composition, respectively.

Summarizing more than 400 compositions of inclusions found mainly in the hook cracks of welded joints, it is proved that they are conglomerates consisting of deoxidation products absorbed on the surface of the refractories of metal wiring. These conglomerates, separated by the onset flow of steel melt from the surface of refractories together with the particles of these refractories, get into the mould, also after the interaction with its slag [19-20]. Such coarse conglomerates cannot penetrate deeply into the solidifying slab, so after its rolling they all find themselves at the edges of the sheet. *This explains the fact why at the edges of the sheet and exactly at close to the bondline the hook cracks form.*

### Results of investigations and discussion

To interpretate chemical composition of NMIs detected in the discontinuities of welded joint defects, we shall consider the possible sources of these inclusions' formation.

#### Sources of exogenous non-metallic inclusions

Approximate compositions of slags and refractory materials, that can be in contact with steel melt during secondary steelmaking and casting, are known from the **Table 1**, which includes elementary composition of these materials in % (wt.) for simplicity of their further comparison with compositions determined in inclusions via SEM-EDS analysis method.

It follows from the Table 1, that slags and refractory materials do not serve as a source of sulfur in non-metallic inclusions, so CaS in their composition should be definitely related to products of steel modification by calcium. The authors of publications [5-10, 18-20] have the same opinion, however, several of them [6-9] have wrongly associated the origin of CaO and Al<sub>2</sub>O<sub>3</sub> in the inclusions found in discontinuities of defects, with exogenous particles of slag. It is impossible to agree with this, since all the slags used during secondary steelmaking and casting still include

SiO<sub>2</sub>, especially in the tundish and mould, where its concentration, calculated on the silicon content, reaches 30% (Table 1).

Thereby only joint presence of CaO, Al<sub>2</sub>O<sub>3</sub> and SiO<sub>2</sub>, as well as MgO and especially alkaline-earth metals can be an identification feature of the origin of these oxides of slags from the tundish and mould. Difference in compositions of these slags can be used for further specification of inclusions. For example, mould powder has 5-10 times more sodium and twice as much potassium than the slag from the tundish. Moreover, mould powder also contains fluorine, and its content of magnesium and aluminum is noticeably lower than in the slag from the tundish (Table 1).

Materials of metal wiring, containing MgO, can be a source of magnesium in exogenous component of non-metallic inclusions (Table 1).

Thus, we considered all possible sources of exogenous component in inclusions that caused the formation of discontinuities in pipe welds, and described their unique identification features by element composition. This approach does not take into account products of secondary oxidation, their presence in composition of inclusions is connected with increased content of Al<sub>2</sub>O<sub>3</sub> [6-9].

**Table 1. Composition of slags and refractory materials, that are in contact with melt during secondary steelmaking and casting**

Slags and refractories	(S)	(Si)	(Al)	(Mg)	(Ca)	Other elements*)
	% (wt.)					
Steel ladle						
Slag	0.1-2.5	1.4-9.8	9.5-18	2.4-13.8	27-44	-
Slag area	-	0.6	0.2	58	0.7	-
Steel area	-	0.6	0.2	58	0.9	-
Bottom	-	0.4	0.2	58	1	-
Impact zone	-	0.8	46.3	4.8	0.3	Ti=1.3
Metal flow from steel ladle into tundish						
Ladle zone	-	-	48.7	3.3	1.6	-
Collector nozzle (contact area with metal)	-	<3.5	<43	3.5	-	Zr=5.9
Protective pipe	-	2.3	>32			C>20
Tundish						
Slag	0.1-0.3	11.7-27.1	2.6-13.2	1.8-4.2	10.7-15.7	Na=0.1-0.3; K=0.1-0.2 Fe=3.5-3.9; F=0.04-0.07
Walls and bottom	-	<2.6	0.2	>51	<2.1	-
Metal receiver	-	2.3	0.2	>48	1.8	-
Metal flow from tundish into mould						
Stopper						
Body	-	9.3	37.6	0.7	0.2	Ti=0.7; Zr=2.2
Nose	-	0.9	2.6	53	0.6	-
Pouring nozzle						
Internal surface	-	3.3	43.4	0.1	0.1	Ti=0.7; Zr=4.3
Surface in slag area	-	3.1	0.4	0.1	2.6	Ti=0.1; Zr=64.4
Seat	-	2	5.2	49	0.6	Zr=0.3
Mould						
Mould powder (MP)	0.05	12.6-29.9	2.6-7.9	0.3-0.7	2.9-27.9	Na=0.4-3.3; K=0.4 Fe=0.2-0.9; F=1-7; C=11-15

\*) Oxygen – balance

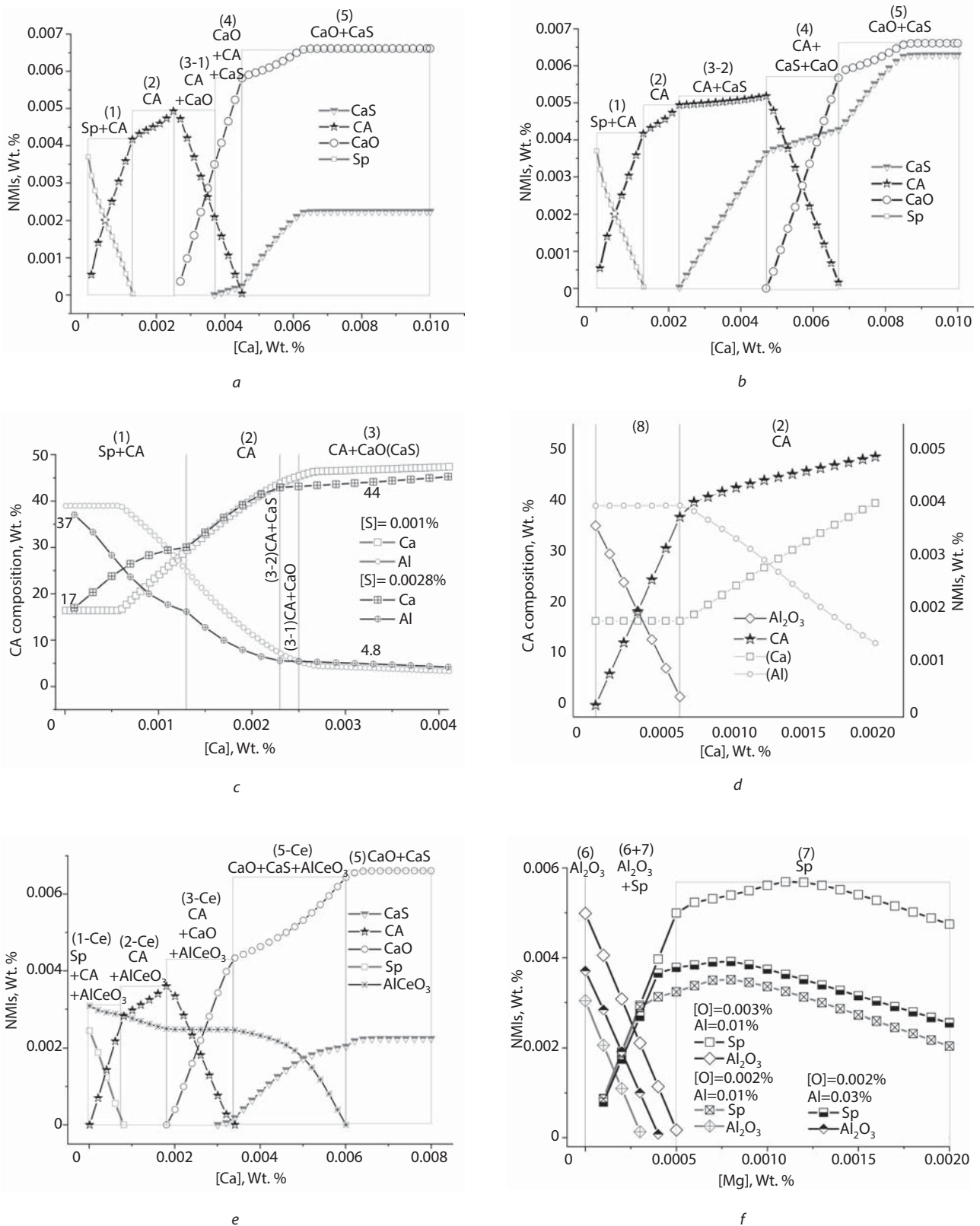


**Fig. 1. Results of thermodynamic simulation of primary NMIs formation for 09G2S steel grade at the temperature 1550 °C.**  
 Steel composition: 0.057 % C, 1.33 % Mn, 0.53 % Si, 0.026 % Al, 0.002 % O<sub>2</sub>, 0 % Mg (f), 0.0005 % Mg (a-c, e), 0.001 % S (a, c-f) and 0.0028 % S (b, c), 0.002 % Ce (e).  
 Symbols of the Fig. 1: Sp – magnesia spinel; CA – calcium aluminates; AlCeO<sub>3</sub> – rare earth metal oxides; (1), (2), (3-1), (3-2), (4), (5), (6), (6+7), (7) and (8) – 10 possible combination of phases in composition of indigenous NMIs, which are formed depending on calcium (a-e) and sulfur (a-c) concentrations for low-alloyed steel modification, or magnesium, oxygen and aluminium (f) during its deoxidation; (1-Ce), (2-Ce), (3-Ce), (5-Ce) and (5) – the same in low-alloyed steel, which was additionally modified by 0.002 % Ce (e)

### Sources of indigenous non-metallic inclusions

Possible combinations of elements in the composition of indigenous NMIs – products of steel deoxidation and modification, formed under the conditions of secondary steelmaking at 1550 °C, can be obtained from the results of thermodynamic simulation. These calculations for low-carbon steels are carried out on the example of 09G2S steel grade, using FactSage 8.0 software, which operates the FSstel and FToxid databases (Fig. 1).

Only primary indigenous NMIs were calculated at the temperature of secondary steelmaking, since these inclusions, formed after deoxidation and modification of steel melt, form conglomerates of NMIs responsible for the formation of defects of welded joints. Secondary NMIs are only 5% of the weight fraction of all products of deoxidation and modification of steel, so they can be ignored. The composition and number of primary inclusions are calculated over a wide range of calcium concentration changes, which is realized in the local dissolution volume of the modifier. If in the melt there is magnesium reduced, for example, from deoxidized steel-ladle slag [18, 21], then with increasing [Ca] in the melt non-metallic inclusions are consequently formed consisting of the following phases: Sp+CA, CA, CA+CaO (at [S]=0.001 % (Fig. 1a)) or CA+CaS (at [S]=0.0028 % (Fig. 1b)), CA+CaO+CaS and CaO+CaS. If magnesium is absent in the melt, then the first pair of phases is formed in the composition  $Al_2O_3$ +CA (Fig. 1d) at [Ca]<0.0006 %, and the rest regions of phase rotation at increasing [Ca] will remain the same as in steel with magnesium (Fig. 1a and Fig. 1b). It should be noted that CA composition in the pair with Sp or with  $Al_2O_3$  (Fig. 1c – 1d) is characterized by higher content of aluminum than calcium, and in the pair CA+CaO or CA+CaS is the contrary: the calcium content in CA is higher than aluminum (Fig. 1c).

When modifying low-carbon corrosion-resistant steels, not only calcium, but also rare-earth metals are used.

The conditions of forming the products of such modification are presented on the Fig. 1e.  $AlCeO_3$  oxides are involved in the following areas: (1-Ce), (2-Ce), (3-Ce) and (5-Ce), while the pair CaO+CaS without  $AlCeO_3$  at [Ca]>0.006 % is formed in the area (5).

Figure 1f shows the formation conditions of deoxidation products at different aluminum content added into steel with different oxygen concentrations. Absence of magnesium leads to forming of  $Al_2O_3$ , when [Mg]<0.0005 % or when [Mg]>0.0005 % - the mixture of  $Al_2O_3$ + $MgO\cdot Al_2O_3$  or single spinel  $MgO\cdot Al_2O_3$  are formed respectively.

Thereby, from the thermodynamic point of view, forming of ten different combinations of phases – deoxidation and modification products – is possible in secondary steelmaking of low-alloyed steel without rare earth metals. All these combinations were revealed in discontinuities of real defects of welded joint of 09G2S steel grade.

### Analysis of NMIs origin in welded joints

Metal discontinuities in welded joint, which was manufactured via high-frequency induction welding from coiled sheet made of 09G2S steel grade and other low-carbon pipe steels, were revealed using ultrasonic control. Polished samples prepared from this metal after etching with a 4% nitric acid solution were examined with Axio Observer D1m inverted microscope equipped with the Thixomet Pro image analysis system. Typical examples of hook cracks in a pipe welded joint after HFIW process are presented on the Fig. 2.

The chemical composition of non-metallic inclusions was determined on unetched cross sections by SEM/EDS analysis methods on JSM-6380LA microscope with the help of X-ray microanalyzer "Analysis Station". The concentrations of all elements contained in the NMIs detected in this way are given in wt. %, where oxygen is the balance up to 100 %.

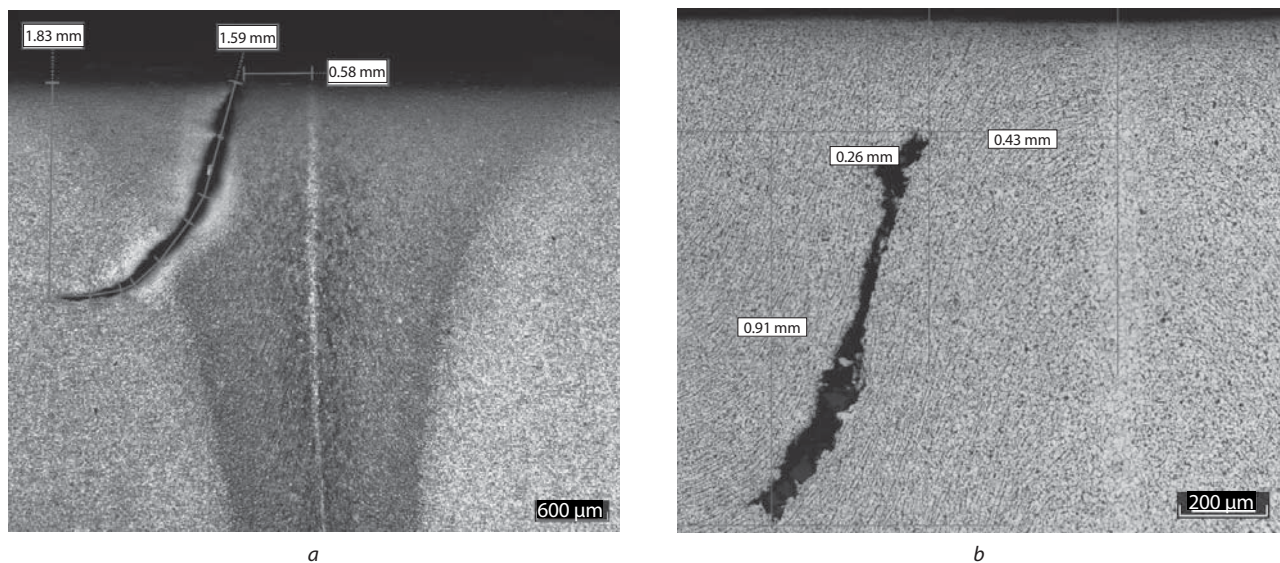


Fig. 2. Example of hook crack defect with exit (a) and without exit (b) on the surface of external pipe diameter

Let us consider the origin of NMIs which were found in discontinuities of hook cracks. Relative part of these cracks in welded joints of pipes manufactured via HFIW technology exceeds 80 %, according to domestic [26] and foreign [4] sources.

### ***Indigenous NMIs – products of steel deoxidation and modification***

This section includes the examples of hook cracks, whose formation was caused by non-metallic inclusions, such as products of steel deoxidation and modification, not containing exogenous component. The examples of such NMIs, which caused the creation of hook-shaped defects, are presented on the Fig. 3.

The pair Sp+CA is formed in aluminum-killed and calcium-modified steel after the interaction of aluminum dissolved in the steel melt with well deoxidized ladle slag [18, 21]. Magnesium reduced from slag participates in the

formation of  $MgO \cdot Al_2O_3$  (Fig. 1a or Fig. 1b); at the same time calcium aluminates in pair with magnesia spinel contain much more Al than Ca (Fig. 3a). The same Al and Ca relationship in CA, as well as the conditions of formation of the pair Sp+CA at  $[Ca] < 0.0013 \%$  are followed from the results of thermodynamic simulations (Fig. 1a – 1c).

Other indigenous NMIs – products of steel modification, which were revealed in discontinuities of hook cracks, are shown on the Fig. 3b – 3d. Figure 3b shows an example where indigenous inclusions liquid CA and solid CaS consist of approximately equal volume fractions at the temperature of secondary steelmaking. As follows from the results of the calculations (Fig. 1b), such a ratio of these phases is formed at higher calcium content in steel (up to 0.0047 %) and  $[S] > 0.0028 \%$ . At the same time, unlike the pair Sp+CA, Ca concentration in calcium aluminates is rather higher than Al concentration (Fig. 3b), what is confirmed by thermodynamic simulations (Fig. 1c).

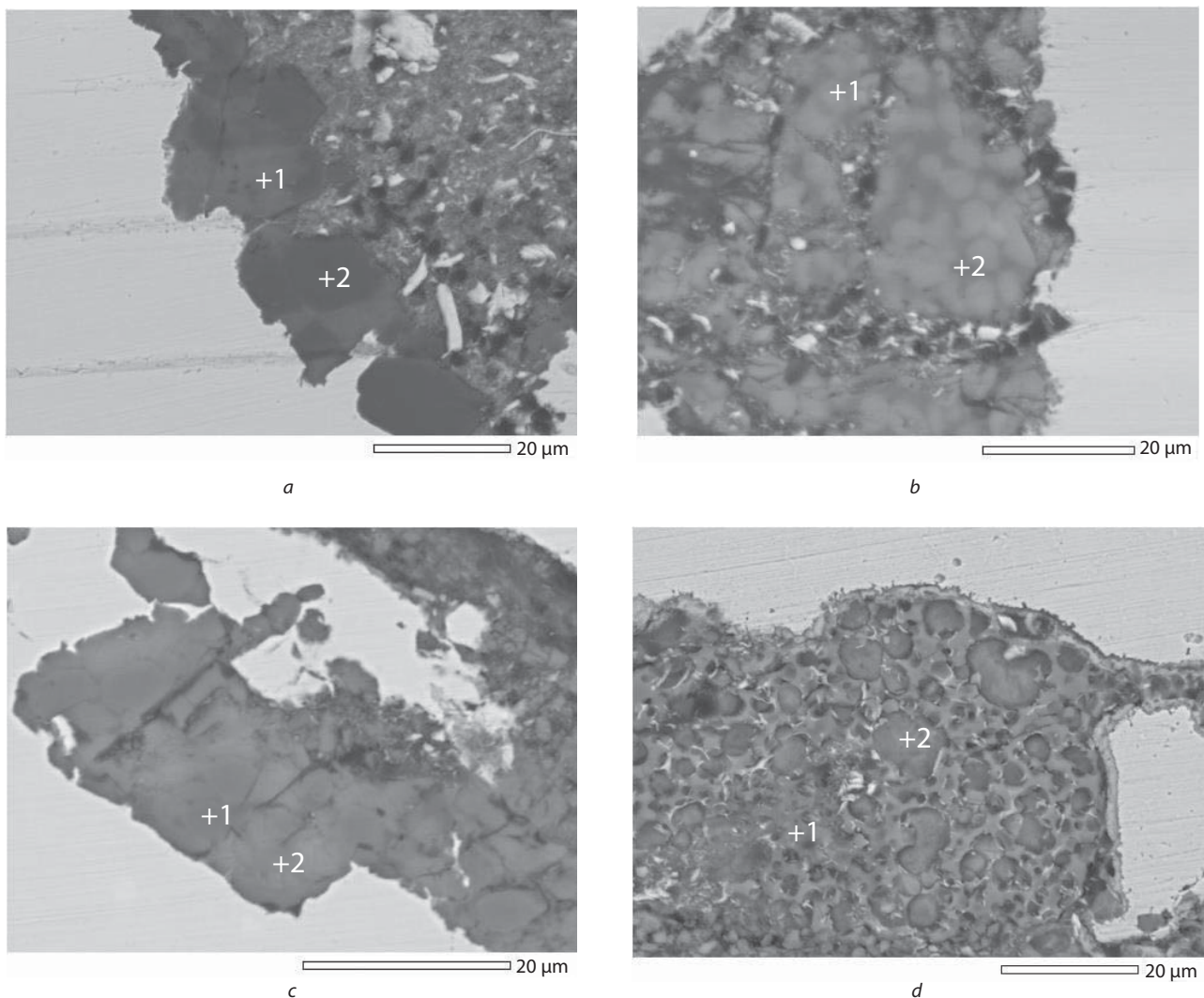


**Fig. 3. Indigenous NMIs— products of deoxidation and modification:**

- a) CA (point 1: 33.5 % Al, 19.4% Ca, 5.2 % Mg), Sp (point 2: 39 % Al, 17.4% Mg);
- b) CaS (point 1: 55 % Ca, 44 % S), CA (point 2: 18 % Al, 41 % Ca, 0.9 % Mg, 4 % S, 2 % Si);
- c) CaO (point 1: 63 % Ca, 0.7 % Mg, 3.6 % S), CaS (point 2: 54.7 % Ca, 36 % S, 1.2 % Al);
- d) CA (point 1: 46.5 % Ca, 12.6 % S, 7 % Al, 1.1% Mg, 0.4 Si, 5 % Ce, 0.7 % La), and CaO (point 2: 52 % Ca, 1 % S).

The example of CaO+CaS pair is presented on the Fig. 3c. As follows from the results of calculations (Fig. 1a and Fig. 1b), depending on the concentration of sulfur in the steel melt, this pair is formed at  $[Ca] > 0.0045-0.0065\%$ , respectively for  $[S] = 0.001-0.0028\%$ . At the same concentration of  $[Ca]$ , the ratio of phases in the area (5) in Fig. 1a and Fig. 1b depends on the concentration of sulfur in the melt:

the more of it, the more CaS and less CaO is formed. At fixed sulfur concentration with increasing calcium content in the melt the fractions of CaO and, especially, CaS increase up to  $[Ca] = 0.0063-0.0085\%$ , respectively at  $[S] = 0.001-0.0028\%$ , and with further increasing of calcium content in the steel melt the fractions of these inclusions do not change. Taking into account the ratio of the CaO and CaS phases (Fig. 3c),

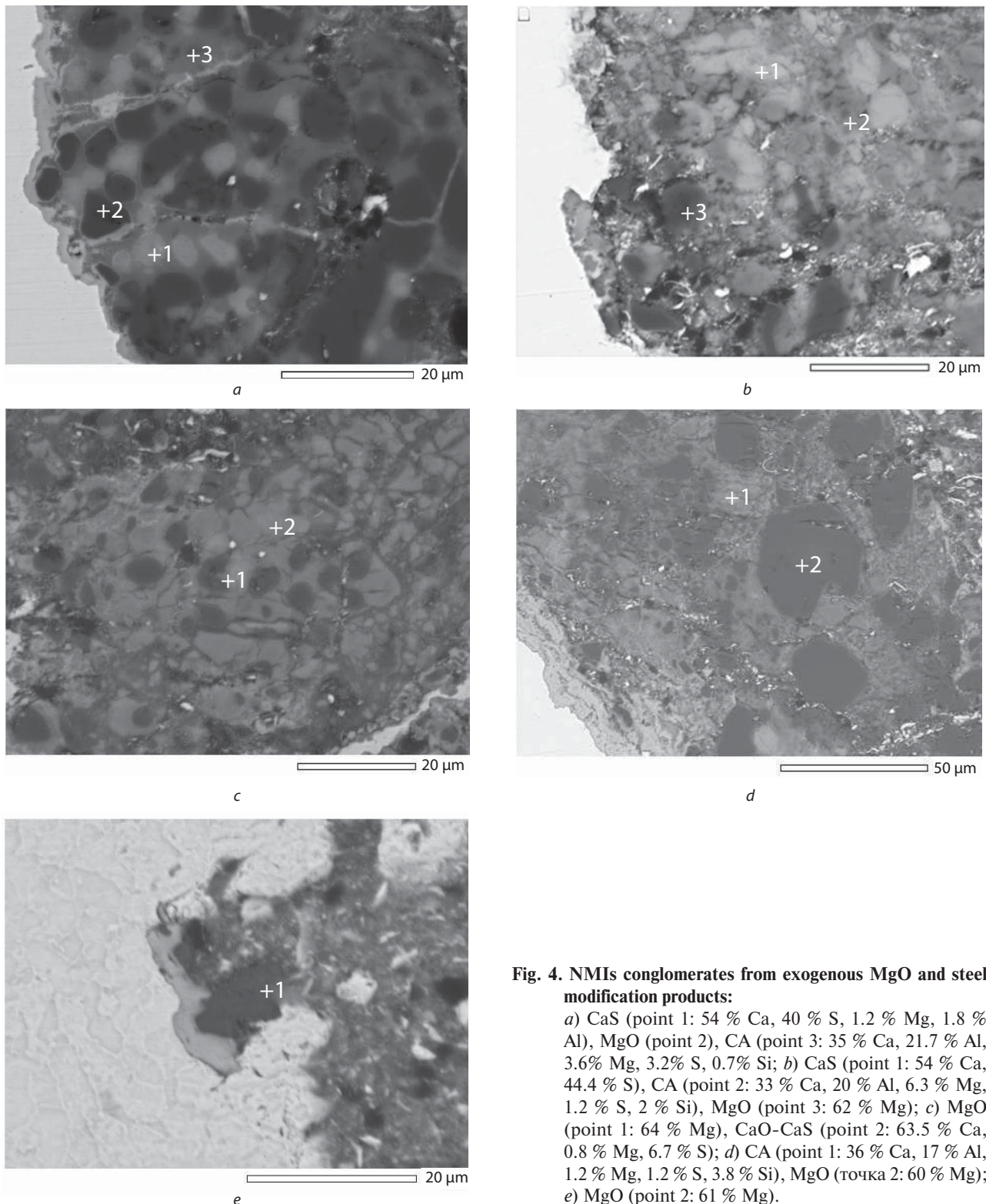


**Fig. 4. NMIs conglomerates from exogenous MgO and steel modification products:**

a) CaS (point 1: 54 % Ca, 40 % S, 1.2 % Mg, 1.8 % Al), MgO (point 2), CA (point 3: 35 % Ca, 21.7 % Al, 3.6% Mg, 3.2% S, 0.7% Si); b) CaS (point 1: 54 % Ca, 44.4 % S), CA (point 2: 33 % Ca, 20 % Al, 6.3 % Mg, 1.2 % S, 2 % Si), MgO (point 3: 62 % Mg); c) MgO (point 1: 64 % Mg), CaO-CaS (point 2: 63.5 % Ca, 0.8 % Mg, 6.7 % S); d) CA (point 1: 36 % Ca, 17 % Al, 1.2 % Mg, 1.2 % S, 3.8 % Si), MgO (точка 2: 60 % Mg); e) MgO (point 2: 61 % Mg).

the conditions of their formation are described by the area (5) on the Fig. 1b, where these phases coexist in approximately equal fractions. Under the same conditions, but after rare earth metals additives, complex inclusions of oxides of rare earth metals, CA, CaS (point 1 in Fig. 3d) and practically pure CaO (point 2 in Fig. 3d) are formed. As follows from the thermodynamic simulations (Fig. 1e), the formation conditions of these compounds are described by the boundary of adjacent areas (3-Ce) and (5-Ce) in Fig. 1e.

#### ***Exo-indigenous NMIs after interaction with MgO***

This section includes the examples of hook cracks formed by exo-indigenous inclusions, which involve MgO-containing refractory particles along with modification products (Fig. 4). These modification products are sorbed on the surface of MgO-containing refractories and react with it, penetrating inside, and then under the influence of onset melt flows in the metal wiring are separated from this surface together with MgO particles.

Attention should be paid to globular form of MgO particles surrounded by calcium aluminates (Fig. 4). The same MgO morphology was observed by the authors of [25], where the impregnation of industrial magnesite refractories with slags of CaO–Al<sub>2</sub>O<sub>3</sub> system was examined. Their results obtained by the sessile drop method displayed that such slags actively penetrate into the open porosity of refractories at the temperature of secondary steelmaking; in this case their surface is destroyed under the action of capillary pressure, while broken off MgO particles are absorbed by slag melt. The paper [25] did not discuss the reasons for the formation of the globular morphology of MgO particles, but it is obvious that after these angular particles are absorbed by the liquid slag, they will begin to spheroidize by the mechanism of Ostwald ripening by recrystallization through liquid phase.

The composition of indigenous component in such conglomerates (Fig. 4a–4d) is almost the same as in the above-considered defects with modification products (Fig. 3). For example, Fig. 4a shows the same as in Fig. 3b, solid CaS and liquid at temperatures of secondary steelmaking calcium aluminates, which penetrate the refractory surface and assimilate MgO particles. Relative fraction of exogenous MgO in the NMIs conglomerate is at least 50 %, and all of them have globular shape and are uniformly distributed in calcium aluminates. This means that the separation of modification products accumulated on the refractories occurred after their deep infiltration and long holding of this semi-solid material. The contact time of modification products with refractory particles was sufficient for almost complete globularization of MgO particles, and the sufficiently low magnesium content of calcium aluminates corresponds to thermodynamic simulations. On the contrary, incomplete globularization and blurred boundary of MgO particles as well as increased Mg concentrations in calcium aluminates (Fig. 4b) testify to the incomplete process of Ostwald ripening of MgO particles.

Fig. 4c shows inclusions which are similar to the previously discussed CaO+CaS indigenous inclusions (Fig. 3c). Difference of exo-indigenous inclusions (Fig. 4c) consists

not only in presence of MgO particles, but also in composition of the indigenous component based on CaO. Thereby the formation conditions of indigenous component of the conglomerate in Fig. 4c correspond to the beginning of the area (5) in Fig. 1a.

It should be noted that a sufficiently large number of globular and uniformly distributed MgO particles indicates a deep infiltration of refractory surface by modification products, while relatively low magnesium content in them indicates the end of the Ostwald ripening processes of these particles.

Calcium aluminates are revealed in the conglomerates in Fig. 4d. The formation conditions of such modification products belong to the area (2) in Fig. 1a or Fig. 1b. The absence of CaO or CaS in the indigenous fraction of conglomerate does not allow us to make a conclusion about the sulfur content in metallic melt from which these aluminates were formed.

Defects, whose source of formation was practically pure exogenous MgO particles, are found in the absence of a liquid phase environment for their Ostwald ripening, their shape leaves angular (fig. 4e).

#### ***Exo-indigenous NMIs after interaction with ZrO<sub>2</sub> and mould powder (MP)***

The formation of this group of defects was caused by deoxidation and modification products after interaction with the surface of ZrO<sub>2</sub>-containing refractory and/or mould powder (Fig. 5).

In contrast to conglomerates of inclusions based on MgO (Fig. 4) in conglomerates of inclusions containing Zr (Fig. 5a–b), pure oxides of this element were not detected, which means the lack of deep infiltration of the ZrO<sub>2</sub>-containing refractory surface by the modification products. However, traces of dissolution of ZrO<sub>2</sub> in the form of separate light bands of Zr-containing phase formed at the end of the oxide melt solidification were found in the products of interaction of CA with refractory. Note that zirconium is localized only in these bands and is not contained in the rest volume of calcium aluminates. Two examples of conglomerates of the same composition, but with different relative fraction of ZrO<sub>2</sub> particles in the composition of NMIs detected in the discontinuities of defects are shown in Fig. 5a and 5b. The longer liquid indigenous inclusions contacted with this refractory, the more ZrO<sub>2</sub> is dissolved in them and the more light bands enriched with this oxide are formed at the end of melt solidification (Fig. 5b). Exactly the same combination, but purely indigenous deoxidation products of Sp+CA, we observed in Fig. 3a, but in contrast to them, in calcium aluminates sorbed on the surface of ZrO<sub>2</sub>-containing refractories, magnesium is not detected (Fig. 5a and 5b). Apparently, Sp is not soluble in calcium aluminates saturated with zirconium oxides.

In the next group of defects, deoxidation or modification products have been in contact with mould powder, including after interaction with ZrO<sub>2</sub>-containing refractory.

Exo-indigenous Al<sub>2</sub>O<sub>3</sub>-based NMIs after interaction with mould powder are shown in Fig. 5c. If we suppose that Al<sub>2</sub>O<sub>3</sub> inclusions have exogenous nature, it is difficult to



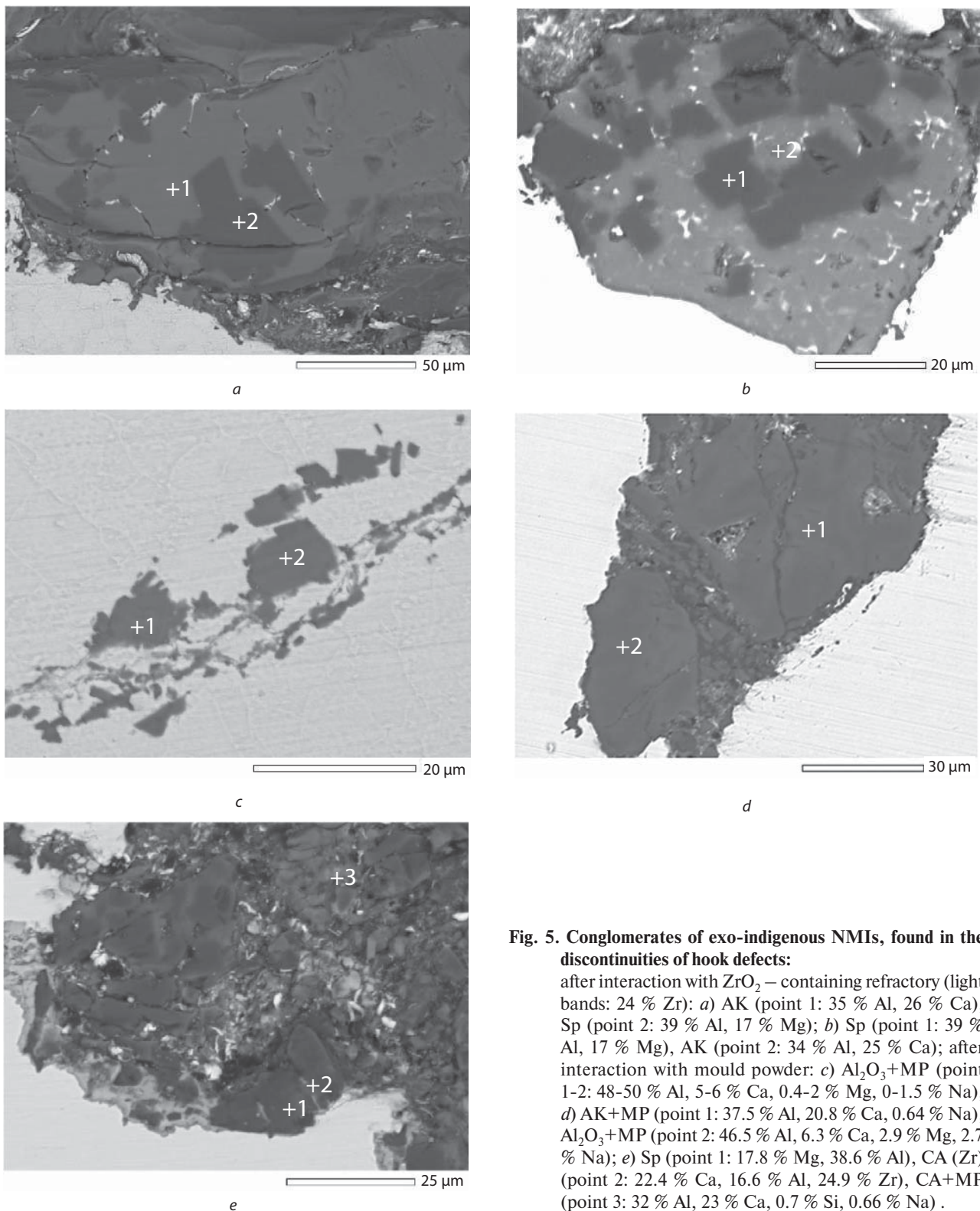


**Fig. 5. Conglomerates of exo-indigenous NMIs, found in the discontinuities of hook defects:**

after interaction with  $ZrO_2$  – containing refractory (light bands: 24 % Zr): *a*) AK (point 1: 35 % Al, 26 % Ca), Sp (point 2: 39 % Al, 17 % Mg); *b*) Sp (point 1: 39 % Al, 17 % Mg), AK (point 2: 34 % Al, 25 % Ca); after interaction with mould powder: *c*)  $Al_2O_3$ +MP (point 1-2: 48-50 % Al, 5-6 % Ca, 0.4-2 % Mg, 0-1.5 % Na); *d*) AK+MP (point 1: 37.5 % Al, 20.8 % Ca, 0.64 % Na),  $Al_2O_3$ +MP (point 2: 46.5 % Al, 6.3 % Ca, 2.9 % Mg, 2.7 % Na); *e*) Sp (point 1: 17.8 % Mg, 38.6 % Al), CA (Zr) (point 2: 22.4 % Ca, 16.6 % Al, 24.9 % Zr), CA+MP (point 3: 32 % Al, 23 % Ca, 0.7 % Si, 0.66 % Na) .

understand how a refractory particle of 10 microns could be absorbed by the melt and remain in its volume during secondary steelmaking and casting of steel, if corundum is not wetted by steel melt. Therefore,  $Al_2O_3$  inclusions are indigenous products of steel deoxidation by aluminum (area (6) in Fig. 1f). These products have been in contact with mould powder, so they contain Na, Ca and Mg.

Exo-indigenous NMIs, which are formed by the pair  $Al_2O_3$ +CA after interaction with mould powder, are shown on the Fig. 5d. It should be noted that, similar to the case with  $MgO$ - $Al_2O_3$  (Fig. 3a, Fig. 5a and 5b), in the contact with  $Al_2O_3$  (Fig. 5d), aluminum concentration in CA is higher than calcium concentration. The same conclusion and conditions of formation of the pair  $Al_2O_3$ +CA at  $[Ca]<0,0006$  % is

followed from the results of thermodynamic simulations (Fig. 1d). Traces of exogenous component after interaction with mould powder (0.64–2.7 % Na) were found in both phases.

The conglomerate of inclusions shown in Fig. 5e involves exogenous components from two sources: one is from  $ZrO_2$ -containing refractory in combination with deoxidation and modification products, and the other is from slag in the mould, in contact with which these exo-endogenous NMIs conglomerates have been in contact.

In this way, 65 and 70 hook cracks were investigated, respectively, in the first and second set of welded joints which obtained in different years. In the discontinuities of these cracks, four main types of NMIs were found, including all ten combinations of indigenous phases predicted by thermodynamic simulation (Fig. 1):

1. Indigenous NMIs (24.3 % / 70 %) – only products of deoxidation (Sp and  $Al_2O_3$ ) and/or modification (Sp, CA, CaO, CaS), including: Sp+CA (10.0 %); CaS+CA (7.1 %); CaO-CaS (2.9 %) and Sp,  $Al_2O_3$ +CA, CaO+CA – 1.4 % of each.

2. Exo-indigenous NMIs – deoxidation and modification products (DMPs), which were sorbed on the surface of MgO-containing refractories (40 % / 26 %), including: MgO+CA+CaS (15.7 %); MgO+CA (14.3 %); MgO-CaO-CaS-CA (5.7 %); MgO+Sp+CA+ $ZrO_2$  (1.4 %) and MgO (1.4 %).

3. Exo-indigenous NMIs – DMPs, which were sorbed on the surface of  $ZrO_2$ -containing refractories (20 % / 0 %), including: Sp+CA+ $ZrO_2$  (18.6 %) and Sp+CA+MP+ $ZrO_2$  (1.4 %).

4. Exo-indigenous NMIs – DMPs and other NMIs after interaction with mould powder (15.7 % / 4 %), including: CA+MP (10.0 %);  $Al_2O_3$ +MP (2.9 %); MgO+CA+MP (2.9 %) and Sp+CA+MP (1.4 %).

The fraction of each of the four main types of NMIs for the second (numerator) and first (denominator) sets is shown in round brackets here. The fractions of different combinations of phases, which are included in composition of the main NMIs types, are noted in round brackets only for the second set.

The above-mentioned statistics were obtained in the analytical module during complex automated analysis of metallographic reports in the Thixomet software [26]. These results are useful for analyzing the current state of production in order to adjust and improve it, as well as to assess trends in its changes in different periods of time. Here are some observations during comparison of defects in the second set with previously examined defects in the first set [26].

The high steel cleanliness in the second set by indigenous NMIs should be noted: the number of defects with only deoxidation and modification products found in their discontinuities, decreased almost three times: from 70 % [26] to 24.3 %. This means that secondary steelmaking in the production of pipes from the second set provided three times more effective elimination of indigenous non-metallic inclusions from liquid steel during argon melt blowing after additives of deoxidizers and modifiers. However, it is known that in the process of argon blowing of steel deoxidized with aluminum, spinel  $MgO-Al_2O_3$  is formed due to the interac-

tion of steel melt with well deoxidized ladle slag. Indeed, if indigenous deoxidation products on the base of spinel caused the formation of only 8 % of all examined defects in the first set [26], number of defects in the second set with  $MgO \cdot Al_2O_3$  tripled to 34.2 %, including Sp+CA (10 %) and Sp+CA+ $ZrO_2$  (18.6 %). With any combination of phases, spinel has always been surrounded by calcium aluminates, so, as we know from the literature, the mechanism of its formation is associated with the reduction of magnesium from the deoxidized ladle slag. Therefore, intensification of mass-exchange processes at the slag-melt boundary during secondary steelmaking, along with the positive effect of removing liquid calcium aluminates into slag, has a negative effect associated with the reduction of magnesium from deoxidized slag and formation of magnesia spinel.

Only one from 65 examined defects in the first set [26] was associated with conglomerates sorbed on the surface of  $ZrO_2$ -containing refractory. The second set had 20 % of such defects, and almost all of them are caused by  $MgO \cdot Al_2O_3$  inclusions with calcium aluminates, which fraction in the second set of defects has increased significantly for the reasons discussed above.

If the number of defects with indigenous products of modification (CA), which contacted with mould powder, was 4 % in the first set, the second set had 15.7 % of such defects; at the same time, deoxidation products ( $Al_2O_3$  and Sp) or Sp+CA combination, as well as CA washed from MgO-containing refractory, were added to modification products. This may indicate a change in assimilating slag abilities in the mould during steelmaking of pipes for the second set.

Thus, the analysis of metallographic reports can be useful for monitoring the current state of production and evaluation of trends in its development, as well as to assess the effectiveness of efforts to improve the technology of secondary steelmaking and steel casting.

The same detailed interpretation was carried out for all kinds of indigenous NMIs in corrosion-resistant, medium-carbon and carbon steel grades, while database “Quality systems of metal products” is equipped with compositions of deoxidation and modification products of steel, formed during their industrial production. It is shown that the same ten combinations of phases, which were predicted by thermodynamic simulation, are formed in the composition of indigenous NMIs that were revealed in discontinuities of pipe welded joints under the existing technological routes of steel deoxidation and modification, independent of steel grade.

## Conclusions

1. On the basis of analysis of foreign experience it is shown that hook cracks are the most common defect of pipe joints obtained by high-frequency induction welding. Especial attention is paid to non-metallic inclusions, which caused the formation of this defect. Their composition, origin and methods of elimination are considered. It is established that the nature of various oxides in NMIs composition revealed in the vicinity of defects is often stated without objective evidence of their origin.

2. Detailed interpretation is given of those NMIs that caused the formation of weld defects, using the data on possible sources of exo- and indigenous inclusions for low-carbon steel grades. All ten combinations of indigenous NMIs revealed in the defects of welded joints of low-carbon steels for the last years, are definitely interpreted by the results of thermodynamic simulations of formation conditions of primary NMIs at 1550 °C. The same detailed interpretation is carried out for all types of indigenous NMIs in corrosion-resistant, medium-carbon and carbon steel grades.


3. New knowledge was established using the data on NMIs composition obtained in industrial reports:

3.1. mechanisms of formation of coarse NMIs conglomerates, consisting of deoxidation and modification products (DMP) mixed with exogenous components from refractories or mould powder. These conglomerates are formed on the surface of refractories of metal wiring and then washed by onset melt flow into the mould during steel casting, in some cases after interaction with mould powder;

3.2. mechanisms of interaction between liquid calcium aluminates with the surface of MgO- and ZrO<sub>2</sub>-containing refractories, which allowed to explain the morphology of exogenous component in conglomerates of these exo-indigenous NMIs;

3.3. regularities of changes in the composition of calcium aluminates, with more aluminum than calcium, if they were formed together with magnesia spinel at [Ca]<0.0013 %, or more calcium than aluminum, if only CA or CA+CaS or CA+CaO or CA+CaO+CaS were formed at [Ca]>0.0013 %;

3.4. regularities of formation of magnesia spinel during secondary steelmaking of the melt modified by calcium; the more calcium aluminates will be removed into the slag during argon melt blowing, the more magnesia spinel will be formed in steel melt.

4. The “Metal products quality system” was developed and implemented on the basis of Thixomet image analyzer, which operates in the laboratories of Vyksa Steel Works. This system enables: to automate the process of generation of metallographic reports; to provide storage of digital information in the database; to process this information to reveal the origin of NMIs, which caused the defects, and to improve the secondary steelmaking and steel casting technologies. 

## REFERENCES

1. Technician ERW Weld Discontinuity Characterization Guide. For the API Long Seam Pipeline (LSP) exam. URL: <https://www.api.org/-/media/Files/Certification/ICP/ICP-Certification-Programs/UT%20Programs/LSP/Technician%20Characterization%20Guide%20for%20API%20LSP%20Exam.pdf?la=en&hash=6A3CA97BDDCE851B0CBBAC81ACCD55311BFC7E21> (access date 06.07.2022).
2. API Bulletin on Imperfection Technology, API Bul. 5T1 (R2017), 2017. 65 p. URL: <https://standards.globalspec.com/std/10185662/api-bull-5t1> (access date 06.07.2022).
3. Fazzini P. G., Cisilino A. P., Otegui J. L. Experimental validation of the influence of lamination defects in electrical resistance seam welded pipelines. *International Journal of Pressure Vessels and Piping*. 2005. Vol. 82. pp. 896–904.
4. Joo M. S., Noh K. M., Kim W. K. et al. A Study of Metallurgical Factors for Defect Formation in Electric Resistance Welded API Steel Pipes. *Metallurgical and Materials Transactions*. 2015. E 2. pp. 119–130. DOI: 10.1007/s40553-015-0049-6 (access date 06.07.2022).
5. Tiratsoo J. Managing pipeline threats. Editor QR 11-9. Hook cracking. URL: <https://pipeline-threats.com/plthreats/qr-11-9-hook-cracking/> (access date 06.07.2022).
6. Sima A. Y., Hossein E., Mehrdad F. Hook crack in electric resistance welding line pipe steel. *Australian Institute for Innovative Materials - Papers*. 2003. 1409. URL: <https://ro.uow.edu.au/ai-impapers/1409>.
7. Ghosh A. Secondary Steelmaking – principles and applications. CRC Press. 2000. 344 p.
8. Kyada T., Raghu Shant J., Goyal D. et al. Analysis of Micro Cracks Near Weld Line in ERW Pipe of API 5L X70M Grade. *Journal of Failure Analysis and Prevention*. 2015. Vol. 15. pp. 344–350. DOI: 10.1007/s11668-015-9950-7.
9. Shin M. H., Han J. M., Lee Y. S., Kang H. W. Study on Defect Formation Mechanisms in ERW for API Steel. *Proceedings of Biennale International Pipeline Conference IPC*. 2014. Vol. 3. 5 p. DOI: 10.1115/IPC2014-33082.
10. Eaves G. N., Cameron S. R., Casey V. J., Nestico P., Bernert W. Hook Crack reduction in ERW line pipe steel. *Steelmaking Conference proceedings*. 1992. pp. 521–528.
11. Tsai H. Thomas. Characterization of Hook Cracks in Tubular Products and Countermeasures 2007. China Iron and Steel – 2007.
12. Sofras Ch., Bouzouni M., Voudouris N., Papaefthymiou S. Investigation of penetrator defect formation during high frequency induction welding in pipeline steels. *MATEC Web of Conf. ICEAF-VI*. 2021. Vol. 349. DOI: 10.1051/mateconf/202134904002.
13. Okabe T., Toyoda S., Goto S., Kato Y., Yasuda K., Nakata K. Numerical Analysis of Welding Phenomena in High-Frequency Electric Resistance Welding. *KEM*. 2014. Vol. 622–623. pp. 525–531. DOI: 10.4028/www.scientific.net/kem.622-623.525.
14. Kaba M., Altay M., Çimenoglu H. An Investigation on the Longitudinal Cracking of Electric Resistance Welded Steel Pipes. *Journal of Failure Analysis and Prevention*. 2020. Vol. 20. pp. 657–662. DOI: 10.1007/s11668-020-00880-3.
15. Kim C. M., Kim J. K. The effect of heat input on the defect phases in high frequency electric resistance welding. *Metals and Materials International*. 2009. Vol. 15. pp. 141–148. DOI: 10.1007/s12540-009-0141-5.
16. GOST 31447–2012. Steel welded pipes for main gas, oil and oil products pipelines. Introduced: 01.01.2015.
17. GOST 59496–2021. Steel welded pipes. Defects of welded joints. Terms and definitions. Introduced: 01.06.2021.
18. Adaba O. et al. An SEM/EDS Statistical Study of the Effect of Mini-Mill Practices on the Inclusion Population in Liquid Steel. *Proceedings of the 9th International Conference and Exhibition on Clean Steel, 2015, Budapest, Hungary*. 2015. September.
19. Kazakov A. A., Murysev V. A., Kiselev D. V. Interpretation of nature of non-metallic inclusions in assessing the quality of metal products in the industrial conditions. *Chernye metally*. 2021. No. 9. pp. 47–54.
20. Kazakov A. A., Murysev V. A., Kiselev D. V. Non-metallic inclusions interpretation technique for factory expertise of metal product defects. *CIS Iron and Steel Review*. 2021. Vol. 22. pp. 41–49. DOI: 10.17580/cisr.2021.02.08.
21. K.C. Ahlberg. *Fifth International Conference on Clean Steel, OMBKE, Budapest, Hungary*. 1997. pp. 151–156.
22. Li Y., Yang W., Zhang L. Formation mechanism of MgO containing inclusions in the molten steel refined in MgO refractory crucibles. *Metals*. 2020. Vol. 10. 444 p. DOI: 10.3390/met10040444.
23. Liu Ch., Gao Xu, Kim S.-J., Ueda Sh., Kitamura Sh. Dissolution behavior of Mg from MgO–C refractory in Al-killed molten steel. *ISIJ International*. 2018. Vol. 58. Iss. 3. pp. 488–495. DOI: 10.2355/isijinternational. ISIJINT-2017-593.
24. Chunyang Liu, Xu Gao, Shigeru Ueda, Muxing Guo, Shin-ya Kitamura. Composition Changes of Inclusions by Reaction with Slag and Refractory: A Review. *ISIJ International*. 2020. Vol. 60. Iss. 9. pp 1835–1848.
25. Wang H., Glaser B., Sichen D. Improvement of Resistance of MgO-Based Refractory to Slag Penetration by In Situ Spinel Formation. *Metallurgical and Materials Transactions B*. 2015. Vol. 46. pp. 749–757. DOI: 10.1007/s11663-014-0277-7.
26. Kazakov A. A., Murysev V. A., Rybalchenko I. V., Stepanov P. P. Non-metallic inclusions and quality of pipe joints obtained by high-frequency electric resistance welding. *Chernye metally*. 2022. No. 6. pp. 60–69.